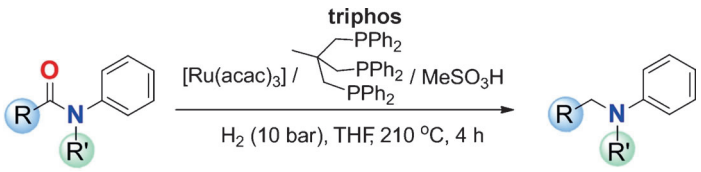

triphos be with you: A homogeneous catalytic system based on complexes prepared in situ from $[Ru(acac)_3]$ and triphos has been developed for the hydrogenation of amides to amines with preservation of the C–N bond (see scheme). This is the first system of any kind that can catalyse the hydrogenation of amides to amines in the presence of aromatic rings without cleavage of the C–N bond.

Homogeneous Catalysis

*J. Coetzee, D. L. Dodds, J. Klankermayer, S. Brosinski, W. Leitner, A. M. Z. Slawin, D. J. Cole-Hamilton** ..... ▮▮▮▮–▮▮▮▮

Homogeneous Catalytic Hydrogenation of Amides to Amines

CHEMISTRY
A EUROPEAN JOURNAL

ChemPubSoc
Europe

DOI: 10.1002/chem.201204270

Homogeneous Catalytic Hydrogenation of Amides to Amines

Jacorien Coetzee,[a] Deborah L. Dodds,[a] Jürgen Klankermayer,[b] Sandra Brosinski,[b] Walter Leitner,[b, c] Alexandra M. Z. Slawin,[a] and David J. Cole-Hamilton*[a]

Abstract: Hydrogenation of amides in the presence of $[Ru(acac)_3]$ (acacH = 2,4-pentanedione), triphos [1,1,1-tris-(diphenylphosphinomethyl)ethane] and methanesulfonic acid (MSA) produces secondary and tertiary amines with selectivities as high as 93% provided that there is at least one aromatic ring on N. The system is also active for the synthesis of primary amines. In an attempt to probe the role of MSA and the mechanism of the reaction, a range of methanesulfonato complexes has been prepared from $[Ru(acac)_3]$, triphos and MSA, or from reactions of [RuX-(OAc)(triphos)] (X = H or OAc) or $[RuH_2(CO)(triphos)]$ with MSA. Crystallographically characterised complexes include: $[Ru(OAc\text{-}\kappa^1O)_2(H_2O)$-(triphos)], $[Ru(OAc\text{-}\kappa^2O,O')(CH_3SO_3\text{-}\kappa^1O)(triphos)]$, $[Ru(CH_3SO_3\text{-}\kappa^1O)_2(H_2O)(triphos)]$ and $[Ru_2(\mu\text{-}CH_3SO_3)_3(triphos)_2][CH_3SO_3]$, whereas other complexes, such as $[Ru(OAc\text{-}\kappa^1O)(OAc\text{-}\kappa^2O,O')(triphos)]$, $[Ru(CH_3SO_3\text{-}\kappa^1O)(CH_3SO_3\text{-}\kappa^2O,O')$-(triphos)], $H[Ru(CH_3SO_3\text{-}\kappa^1O)_3$-(triphos)], $[RuH(CH_3SO_3\text{-}\kappa^1O)(CO)$-(triphos)] and $[RuH(CH_3SO_3\text{-}\kappa^2O,O')$-(triphos)] have been characterised spectroscopically. The interactions between these various complexes and their relevance to the catalytic reactions are discussed.

Keywords: amide hydrogenation · amines · catalysis · homogeneous catalysis · ruthenium

Introduction

We report the first successful homogeneous catalysts for the hydrogenation of amides to amines with preservation of the C–N bond. This is also the first system of any kind that can catalyse the hydrogenation of amides to amines in the presence of aromatic rings without cleavage of the C–N bond. Many active pharmaceutical compounds contain an amine functionality, which is often introduced by the formation and subsequent reduction of an amide using $LiAlH_4$ or borane reducing agents. These reducing agents, however, are not only pyrophoric and difficult to handle but also involve complex work-up procedures while generating large amounts of waste. These factors make their use on large scale problematic. Using catalytic hydrogenation would be an ideal solution to the problem since water is produced as the only by-product. Attempted amide hydrogenations using homogeneous catalysts have been reported by the groups of Milstein, Saito and Bergens, but they either lead to C–N bond cleavage to give alcohols and amines[1] or to hemiaminals by monohydrogenation.[2] Although some heterogeneous hydrogenation catalysts have been reported to give good conversions of amides to amines, they generally require harsh operating conditions while only displaying moderate to poor selectivity.[3] In addition, their use is mostly limited to substrates devoid of aromatic ring systems, since unwanted ring hydrogenation represents a major side reaction. More recently, a bimetallic Pt/Re-based catalyst capable of promoting amide hydrogenations under milder conditions has been reported by Burch et al.[4] However, we have found the use of this system to be limited to non-aromatic substrates owing to the occurrence of unwanted ring hydrogenation.[5] While this paper was under review, a system using Pd/Re on graphite was reported. A wide range of amides are hydrogenated to amines under mild conditions, but once again, aromatic rings in the substrates are also hydrogenated.[6]

Catalytic hydrosilylation represents an interesting alternative for amide reductions and has been shown to proceed under mild reaction conditions whilst displaying good functional group tolerance.[7] Despite the wider substrate scope, hydrosilylation reactions still proceed with lower atom efficiency than more classical hydrogenations involving molecular hydrogen. Thus, selective and environmentally benign amide hydrogenation reactions are rare and for this reason the American Chemical Society Green Chemistry Institute (GCI) and members of the Pharmaceutical Round Table have identified amide hydrogenation as one of their three most desirable reactions for development.[8]

[a] Dr. J. Coetzee, Dr. D. L. Dodds, Prof. A. M. Z. Slawin, Prof. D. J. Cole-Hamilton
EastChem, School of Chemistry
North Haugh, University of St. Andrews
St. Andrews, Fife, KY16 9ST, Scotland (UK)
E-mail: djc@st-andrews.ac.uk

[b] Prof. J. Klankermayer, S. Brosinski, Prof. W. Leitner
Institut für Technische und Makromolekulare Chemie
RWTH Aachen University, Worringerweg 1
52074 Aachen (Germany)

[c] Prof. W. Leitner
Max-Planck-Institut für Kohlenforschung, Kaiser-Wilhelm-Platz 1
45470 Mülheim a.d. Ruhr (Germany)

Supporting information for this article is available on the WWW under http://dx.doi.org/10.1002/chem.201204270.

Our new amide hydrogenation catalysts, which keep the C–N bond intact, are based on complexes prepared in situ from [Ru(acac)$_3$] and 1,1,1-tris(diphenylphosphinomethyl)-ethane (triphos), a system which is known to be active for the hydrogenation of carboxylic acids and esters.[9] We also describe other precatalysts, the role of acid and discuss the possible active species present during the reactions. Some of these results have been communicated in preliminary form.[10]

Results and Discussion

[Ru(acac)$_3$]/triphos system in catalytic amide reductions: Heating benzanilide (**1**, R = R′ = Ph) in THF in the presence of [Ru(acac)$_3$] (1 mol %), triphos (2 mol %) and methanesulfonic acid (1 mol %) to 220 °C under hydrogen (40 bar at RT, pressure at the reaction temperature is ca. 70 bar) for 16 h smoothly produces *N*-benzylaniline (**3**, R = R′ = Ph) with 88 % selectivity. The other products are small amounts of dibenzylaniline (**6**, R = R′ = Ph), aniline (**4**) and *N*-benzylideneaniline (**2**, R = R′ = Ph; Table 1, entry 1). The proposed origin of these products is shown in Scheme 1, which summarises the reduction and transamination reactions.

For benzanilide, full conversion can be achieved in 8 h and the selectivity towards the desired secondary amine improved by working at lower pressures (Table 1, entry 2). Reducing the [MSA] to 0.5 mol % makes little difference (Table 1, entry 3), but too much acid is detrimental since the major products become **6** (R = R′ = Ph) and *N*-phenylpyrrolidine (Table 1, entry 4), presumably formed from the acid catalysed reaction of aniline with the solvent THF. The pressure can be dropped to 5 bar but a longer reaction time is required and more **6** (R = R′ = Ph) is produced (Table 1, entry 5), presumably because transamidation of **1** (R = R′ = Ph) with the product **3** (R = R′ = Ph) competes more effectively with the slower hydrogenation of **1** (R = R′ = Ph). Adding aniline in an attempt to suppress transamidation, makes little difference to the reaction selectivity (Table 1, entry 7). The nature of the autoclave is also important. Hastelloy^{TM} C is ideal whereas stainless steel tends to lead to products in which the phenyl rings are hydrogenated. This suggests that metallic ruthenium or nanoparticles, known catalysts for the hydrogenation of aromatic rings, may form (Table 1, entry 6), although we have not explored this in detail. The use of a glass liner in a stainless steel autoclave alleviates this problem and allows successful reactions.

Very similar chemistry is observed when using *N*-phenylacetamide as substrate (**1**, R = Me; R′ = Ph) and it was shown, by working at constant pressure and monitoring gas uptake from a ballast vessel, that the reaction at 10 bar (RT, 40 bar at the reaction temperature) and 200 °C is complete within 2 h. The effect of added acid is shown in Figure 1,

Table 1. Hydrogenations of benzanilide (**1**, R = R′ = Ph) with [Ru(acac)$_3$]/triphos and catalytic amounts of MSA.[a]

Entry	P_{H_2} [bar][b]	MSA [mol %]	*t* [h]	**2** [%]	**3** [%]	**4** [%]	**6** [%]	Conv. [%]	Sel. [%]
1	40	1	16	2	85	3	10	100	88
2	10	1	8	3	93	0	4	100	93
3	10	0.5	16	3	92	0	5	100	92
4[c]	10	10	16	<1	12	0	28	100	12
5	5	0.5	62	4	78	5	13	100	82
6[d]	10	1	16	ring hydrogenation products observed					
7[e]	10	1	16	2	91	0	7	100	91

[a] Conditions: amide (5 mmol), [Ru(acac)$_3$] (1 mol %), triphos (2 mol %), THF (10 mL), 220 °C, Hastelloy^{TM} autoclave. Calculations based on GC-FID; selectivity is **3**/(**2**+**3**+**6**). [b] At RT. [c] *N*-Phenylpyrrolidine, benzylbenzamide and two other impurities are also formed, they are included as products in the calculation of selectivity. [d] Stainless steel autoclave. [e] Aniline (1 %) added.

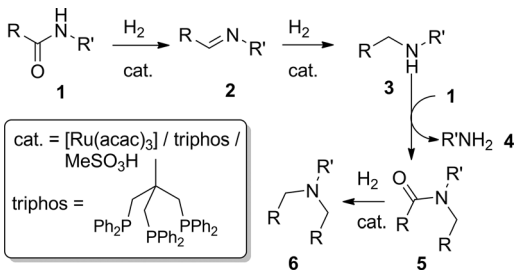

Scheme 1. Origin of the various products observed during the catalytic hydrogenation of amides.

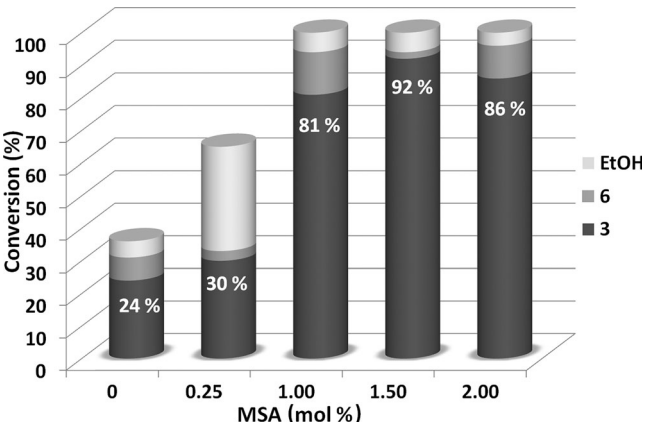

Figure 1. Effect of [MSA] on the products of *N*-phenylacetamide hydrogenation. *N*-phenylacetamide (**1**, R = Me; R′ = Ph, 5 mmol), [Ru(acac)$_3$] (1 mol %), triphos (2 mol %), 210 °C, H_2 (10 bar), THF, (10 mL), 16 h; for **6** and **3** R = Me and R′ = Ph.

with the selectivity towards the desired secondary amine, *N*-ethylaniline (**3**, R = Me; R′ = Ph), increasing with added acid at least to 1.5 mol % (selectivity 92 %). In these reactions, ethanol is the major by-product. This is presumably formed by hydrogenation of acetic acid, the amide hydrolysis product formed from the water generated in the reaction.

Changes in the reaction temperature also greatly affect the catalytic hydrogenation of *N*-phenylacetamide, with internal temperatures below 120 °C leading to limited conversion with zero selectivity towards the desired amine (Figure 2). At temperatures above 150 °C, full conversion is

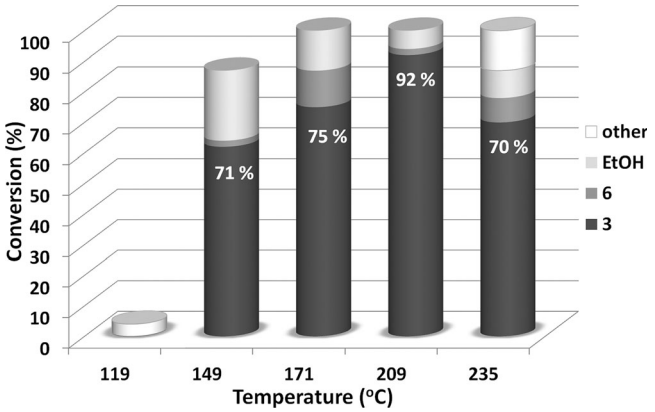

Figure 2. Effect of increasing temperatures on the products of hydrogenation of *N*-phenylacetamide, where "other" refers to ring hydrogenated products. *N*-Phenylacetamide (**1**, R = Me; R′ = Ph, 5 mmol), [Ru(acac)$_3$] (1 mol %), triphos (2 mol %), MSA (1.5 mol %), 120–235 °C, H_2 (10 bar), THF (10 mL), 16 h; for **6** and **3** R = Me and R′ = Ph.

achieved with the selectivity towards *N*-ethylaniline (**3**, R = Me; R′ = Ph) reaching a maximum (92 %) at around 210 °C. At even higher temperatures, catalyst decomposition starts to become important with the metallic Ru generated leading to the formation of unwanted ring hydrogenated products (other in Figure 2). A hydrogenation of *N*-phenylacetamide carried out at 200 °C, under H_2 (10 bar) using MSA (1.5 mol %) gave comparable results in the presence and absence of added mercury, suggesting that, at least up to 200 °C, the reaction is homogeneous (Table 2, footnote [e]).

The substrate scope for the catalytic hydrogenation of primary, secondary and tertiary amides using the [Ru(acac)$_3$]/triphos system is summarised in Table 2. It is clear from the results obtained with secondary and tertiary amides that the reaction works with high selectivity if there is a phenyl group on nitrogen. There does not seem to be a correlation between reaction selectivity and the electron density on the *N*-aromatic ring. In some cases, for example, with *N*-methylbenzamide (**1**, R = Ph; R′ = Me; Table 2, entry 2), although the selectivity to the desired secondary amine is poor, the major product is dibenzylmethylamine (**6**, R = Ph; R′ = Me).

In the mentioned case, the hydrogenation works, but slowly compared with the rate of transamidation. Similar arguments apply to the hydrogenation of *N*-benzylacetamide (**1**, R = Me; R′ = Bz; Table 2, entry 18). In both cases, minor products observed have scrambling of the alkyl/aryl groups on the amine product. The only secondary amide substrates we have examined with which reactivity is poor are *N*-(2-chlorophenyl)acetamide, *N*-(4-chlorophenyl)acetamide and *N*-benzyl-4-methylbenzamide (Table 2, entries 9, 11 and 14) and *N*-(4-nitrophenyl)acetamide, with which substantial catalyst decomposition occurs leading to preferential hydrogenation of the ring and the nitro group (Table 2, entry 12).

When using tertiary amide substrates, the yields of amine are generally poor—in some cases because the reaction is slow, whereas in others because the selectivity is poor. Similar to the secondary amides, reactions again proceed better if there is an aromatic group on N. Finally, the primary amide butanamide gives mainly secondary and tertiary amines in the absence of ammonia, as previously found for reactions carried out in the absence of acid,[9c,10a] but gives the primary amine butylamine as the major product when the reaction is carried out in the presence of aqueous ammonia (Table 2, entry 1).

In order to be sure that the reactions were genuinely reproducible between laboratories, hydrogenations of *N*-phenylacetamide were carried out at RWTH Aachen University using the optimised conditions from the St. Andrews laboratory (Table 3). At 10 bar hydrogen pressure, only 51 % conversion was obtained after 16 h due the limited amount of hydrogen present in the 10 mL autoclave containing a glass liner (Table 3, entry 1). Increasing the hydrogen pressure stepwise to 75 bar resulted in full conversion of the *N*-phenylacetamide (Table 3, entries 2–5). The importance of a sufficient amount of acidic additive and triphos in the catalytic reaction is demonstrated in the reduced conversion of 87 % with only 1 mol % MSA and triphos (Table 3, entry 6). In most of the reactions the selectivity towards **3** (R = Me; R′ = Ph) is >90 %. Small amounts of ethanol and **6** (R = Me; R′ = Ph) represent the major by-products.

In situ NMR studies: In order to elucidate the formation of the actual precatalyst from the in situ system, variable temperature high pressure NMR (VT-HP NMR) experiments were conducted. Solutions of [Ru(acac)$_3$] (10 mol %), triphos (20 mol %) and *N*-phenylacetamide in degassed [D$_8$]THF were transferred to a sapphire high pressure NMR cell under a H_2 atmosphere and then pressurised to 10 bar with H_2 in the absence and presence of MSA (1.5 mol %). Surprisingly, even at the maximum probe temperature of 130 °C, the measured ^{1}H and ^{31}P{^{1}H} NMR spectra of both solutions showed very little difference from those of the starting materials, suggesting that the reduction of Ru^{III} to Ru^{II} with concurrent triphos coordination does not proceed as readily as was first anticipated. Therefore, a solution of [Ru(acac)$_3$], triphos (2 equiv) and MSA (1.5 equiv) in THF was pressurised to 10 bar with H_2 in a Hastelloy™ autoclave and heated for 4 h at 210 °C. ^{31}P{^{1}H} NMR analysis of the crude product mixture indicated, in addition to oxidised triphos (resulting from the reduction of Ru), a mixture of fluxional species giving rise to a broad resonance around δ_P = 40 ppm. From low temperature ^{31}P{^{1}H} NMR spectra, it is evident that the fluxional mixture consists of a number of new species (Figure 3). As outlined in the next sections, the majority of these species could be identified and structurally characterised through the investigation of the reactivity and catalytic performance of preformed precatalysts in the presence and absence of MSA.

Preformed precatalysts: Since an Ru^{II}–triphos unit seems likely to be the basis of the active site during the catalytic cycle, special focus was placed on Ru complexes already containing this motif (Figure 4). Of the tested precatalysts **7**–**10**, only **9** and **10** displayed catalytic activity towards the

Table 2. Substrate scope for amide hydrogenations with the [Ru(acac)$_3$]/triphos system.[a]

Entry	Substrate	MSA [mol%]	T [°C]	P_{H_2} [bar]	Conv. [%]	Sel. [%]	Entry	Substrate	MSA [mol%]	T [°C]	P_{H_2} [bar]	Conv. [%]	Sel. [%]
Primary amide[b]													
1	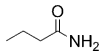	1.5	200	10	100	61							
Secondary amides													
2	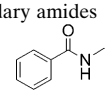	1.5	200	10	82[c]	<5[c]	11		1.5	200	10	45	0
3	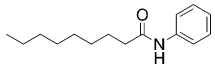	1.5	200	10	92[d]	92[d]	12	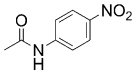	1.5	200	10	100	0
4		1.5	200	10	100[e]	92[e]	13	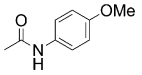	1.0	220	10	97	78
5	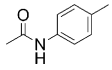	1.0	220	10	98	78	14	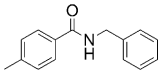	1.5	200	10	15[f]	<5[f]
6	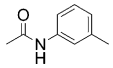	1.5	200	10	100	79	15	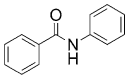	1.0	220	10	100	92
7		1.5	200	10	100	90	16	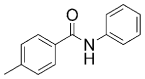	1.5	200	10	100	94
8	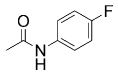	1.0	220	10	99	77	17	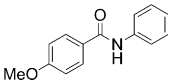	1.5	200	10	92[c]	61[c]
9	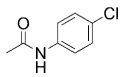	1.5	200	10	64	28	18	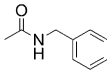	1.5	220	10	100	<5
10	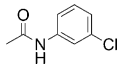	1.5	200	10	75	75							
Tertiary amides													
19	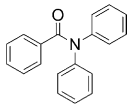	1.5	220	10	92	73	22	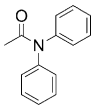	1.0	220	40	83	42
20	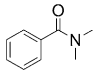	1.5	220	10	33[c]	7[c]	23		1.5	200	10	19	100
21		1.5	200	10	19	63	24		1.5	200	10	0	0

[a] Conditions: substrate (5 mmol), [Ru(acac)$_3$] (1 mol%), triphos (2 mol%), THF (10 mL), 16 h. Conversion and selectivity were calculated using NMR integration. [b] Reaction performed in the presence of aq. NH_3 (10 mL). [c] Based on uncalibrated GC-FID integration. [d] Ref. [6] reports 87% conv. and 78% sel. [e] Selectivity for different reactions with *N*-phenylacetamide under identical conditions varies between 86–92%. In the presence of added mercury, 100% conversion with 84% selectivity was obtained. [f] Small amounts of mixed tertiary amines formed.

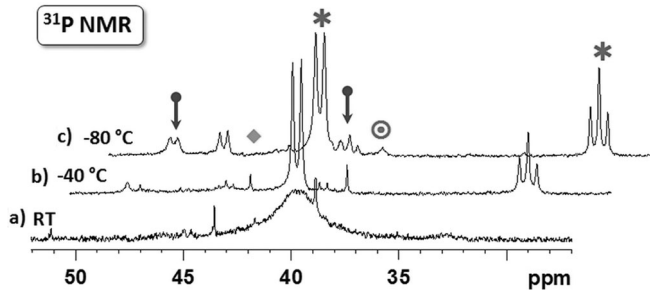

Figure 3. Variable temperature $^{31}P\{^1H\}$ NMR spectra of the complex mixture obtained when [Ru(acac)$_3$] is treated with triphos and MSA (1.5 equiv) under a H_2 pressure of 15 bar at 210°C for 4 h. Markers (thin arrow, dot in circle, diamond and star) indicate distinct species that will be identified (vide infra).

hydrogenation of *N*-phenylacetamide under the conditions typically employed for the conventional [Ru(acac)$_3$]/triphos system. Under these conditions, **9** gave full conversion of **1** (R = Me, R′ = Ph), but with a slightly lower selectivity of 78% towards **3** (R = Me, R′ = Ph). The hydrogenation of *N*-phenylacetamide in the presence **9** was explored over a range of temperatures with the results summarised in Table 4. Catalyst **9** performed rather poorly at lower temperatures when compared with [Ru(acac)$_3$]/triphos under the same conditions (Figure 2). It can thus be concluded that the high temperatures required for these transformations are not solely associated with initial Ru^{III} reduction and triphos coordination but are also required for the turnover of the catalytic cycle itself.

Table 3. Catalytic hydrogenation of *N*-phenylacetamide with $[Ru(acac)_3]$/triphos in 10 mL autoclave.[a]

Entry	triphos [mol%]	MSA [mol%]	P_{H_2} [bar][b]	*t* [h]	Conv. [%]	Sel. [%]
1	2	1.5	10	16	51	91
2	2	1.5	30	16	90	90
3	2	1.5	50	16	97	88
4	2	1.5	75	24	>99	92
5	2	1.5	75	16	>99	90
6	1	1	75	24	87	87

[a] Conditions: *N*-phenylacetamide (**1**, R = Me; R′ = Ph, 0.25 mmol), $[Ru(acac)_3]$ (1 mol%), 200 °C, stainless steel autoclave (10 mL) with a glass liner. Selectivity is **3**/(**3**+**6**+[EtOH]); for full product analysis see the Supporting Information. [b] Pressure at RT.

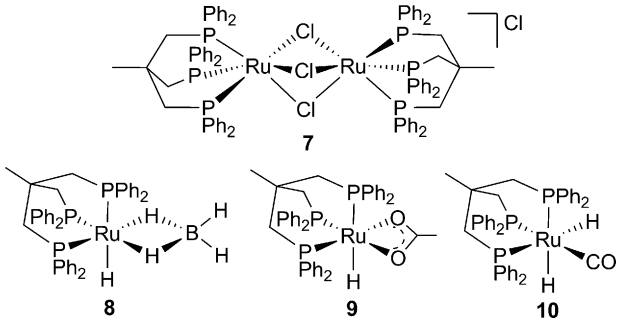

Figure 4. Preformed precatalysts **7**–**10** tested for catalytic activity in amide hydrogenation reactions with *N*-phenylacetamide.

Table 4. Catalytic hydrogenation of *N*-phenylacetamide with **9** as precatalyst over a range of temperatures.[a]

Entry	*T* [°C]	**3** [%]	**6** [%]	EtOH [%]	Other [%]	Conv. [%]	Sel. [%]
1	120	0	0	1	26	27	0
2	150	0	0	1	99	100	0
3	200	75	23	0.4	1.6	100	75
4	210	78	11	0.5	10.5	100	78
5[b]	210	60	10	13	0	83	73

[a] Conditions: *N*-phenylacetamide (**1**, R = Me; R′ = Ph, 5 mmol), [RuH(OAc-κ^{2}O,O′)(triphos)] (**9**, 1 mol%), MSA (1.5 mol%), THF (10 mL), H_2 (15 bar at RT), 16 h in a Hastelloy™ autoclave (250 mL); selectivity is **3**/(**3**+**6**+[EtOH]); for full product analysis see the Supporting Information. [b] Performed in the absence of added MSA.

$^{31}P\{^1H\}$ NMR analysis of the final product mixture obtained for hydrogenations with **9** at various reaction temperatures, indicated the presence of two major species. Interestingly, at lower reaction temperatures an unknown species giving rise to a triplet at $\delta_P = 28.4$ ppm and a doublet at $\delta_P = 45.3$ ppm was prevalent, whereas at higher temperatures the known complex, $[Ru(H)_2CO(triphos)]$ (**10**),[9g] constituted the major species ($\delta_P = 26.9$ ppm (d) and $\delta_P = 35.2$ ppm (t); Figure 5). The latter has also been reported by some of us to be present at the end of catalytic hydrogenations using $[Ru(acac)_3]$/triphos with carboxylic acids as substrate, and has been shown to be formed by the decarbonylation of aldehydes.[9f,g] Although aldehydes cannot be produced by any

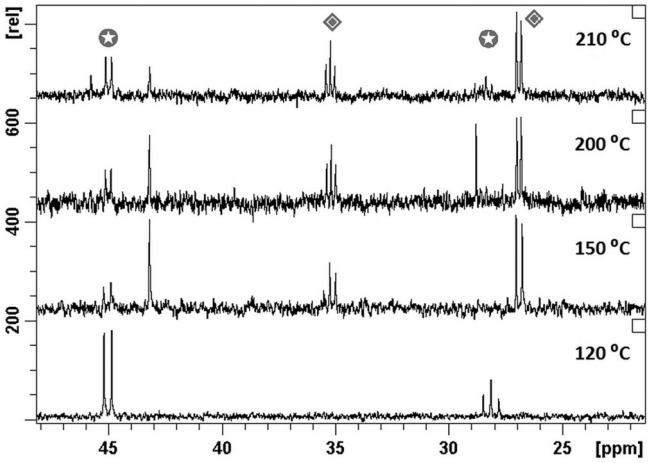

Figure 5. Comparison of the $^{31}P\{^1H\}$ spectra (CD_2Cl_2, 25 °C) recorded for the crude product mixtures obtained after catalytic hydrogenation of *N*-phenylacetamide with **9** at various temperatures, displaying mainly resonances corresponding to $[Ru(H)_2CO(triphos)]$ (**10**; diamond) and an unknown species (star in circle).

direct routes when *N*-phenylacetamide is the substrate, acetic acid and ethanol are produced as side products and are plausible sources for the carbonyl group. As mentioned, **10** is itself a precatalyst for the hydrogenation of acetanilide.

To add to our understanding of the role of methanesulfonic acid in the catalytic system, a solution of **9** in THF was treated with either 1 or 2 equiv of MSA at RT and the resulting reaction products were analysed by NMR spectroscopy. With the addition of only 1 equiv of MSA, the hydride ligand in **9** is lost to form hydrogen with the formation of the mono-substituted complex $[Ru(CH_3SO_3)(OAc\text{-}\kappa^2O,O')(triphos)]$ (**11**) as the only product (Scheme 2 (a)). Interestingly, in the presence of 2 equiv of MSA, a mixture of three complexes, $[Ru_2(\mu\text{-}CH_3SO_3)_3(triphos)_2]CH_3SO_3$ (**12**), $H[Ru(CH_3SO_3\text{-}\kappa^1O)_3(triphos)]$ (**13**) and $[Ru(CH_3SO_3\text{-}\kappa^1O)(CH_3SO_3\text{-}\kappa^2O,O')(triphos)]$ (**14**) is initially obtained (Scheme 2 (b)). An equilibrium, which lies towards the thermodynamically more stable monomeric **14**, exists between these compounds (Scheme 2 (c)). The assignment if **12** has been confirmed by isolation and crystallographic characterisation (Figure S5 in the Supporting Information). The structure of **13** is tentatively assigned from its low temperature NMR spectrum, its predominance when excess MSA is present and its fluxionality presumably arising from the proton moving between pairs of methanesulfonato ions. Similarly, **14** is tentatively assigned from its low temperature $^{31}P\{^1H\}$ NMR spectrum. Attempted crystallisation of **13**/**14** gave $[Ru(CH_3SO_3\text{-}\kappa^1O)_2(H_2O)(triphos)]$ (**19**; Figure S6 in the Supporting Information).

In the $^{31}P\{^1H\}$ NMR spectrum of the mixture run immediately after it was isolated, **12** is detected as a sharp singlet at $\delta_P = 38.5$ ppm whereas the fast exchanging **13** and **14**, which could only be assigned tentatively, are only observed by an averaged broad singlet with a chemical shift $\delta_P = 40.7$ ppm (Figure S1b in the Supporting Information) in between that of **13** ($\delta_P = 48.5$ ppm; Figure S1a in the Supporting Informa-

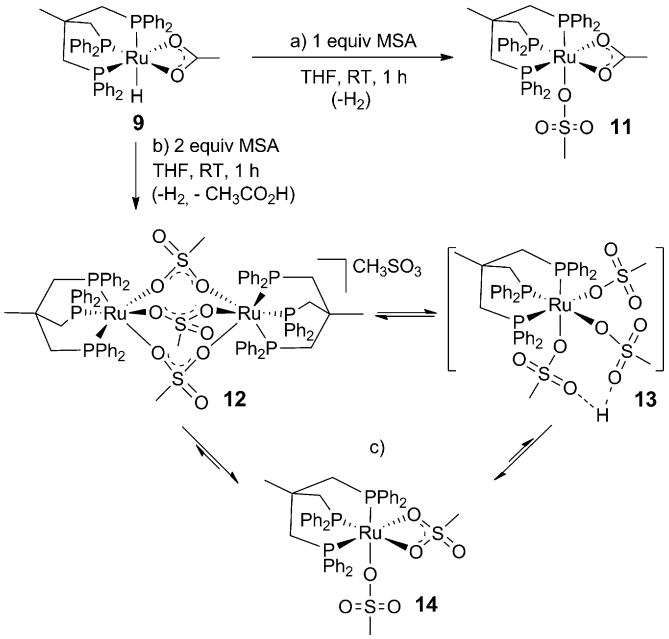

Scheme 2. Reaction products observed when treating **9** with either: a) 1 equiv, or b) 2 equiv of MSA.

tion) and **14** ($\delta_P = 38.7$ ppm; Figure S1c in the Supporting Information). A $^{31}P\{^1H\}$ NMR spectrum taken of this mixture after some time in solution, however, shows the change in the composition to give largely what we propose to be **14** at the expense of **12** and **13** (Figure S1c in the Supporting Information). Compound **13** can be obtained as the major species in the presence of a large excess of MSA (>3 equiv) and is also the predominant product if [Ru(OAc-κ^1O)(OAc-κ^2O,O′)(triphos)] (**15**) is treated with a large excess of MSA. We thus propose it to be H[Ru(CH_3SO_3-κ^1O)$_3$triphos] as the $^{31}P\{^1H\}$ NMR analysis of **13** frozen out at −80 °C displayed a triplet at $\delta_P = 41.1$ ppm and a doublet at $\delta_P = 50.0$ ppm ($^2J_{PP} = 42.6$ Hz). This profile presumably arises because the acidic proton is hydrogen bonded between only two of the $[CH_3SO_3]^-$ groups at low temperatures (Scheme 2), whilst migrating between all three groups at higher temperatures. The structures of **11** and **12** could be confirmed by single crystal X-ray diffraction and are discussed in more detail in the Supporting Information (Figures S4 and S5).

The behaviour of these species in the presence of substrate and hydrogen was assessed by VT-HP NMR spectroscopy. Addition of MSA (15 mol%) to a solution of *N*-phenylacetamide (0.75 mmol) and **9** (10 mol%) in [D_8]THF (3 mL) resulted in the immediate evolution of hydrogen gas. The RT $^{31}P\{^1H\}$ NMR spectrum of this solution under a H_2 pressure of 10 bar displays a mixture of fluxional species in the form of a series of broad resonances within the region $\delta_P = 48$–38 ppm (Figure S2a in the Supporting Information). At higher temperatures, the rate of exchange is increased until finally all species are observed as a single averaged broad singlet at $\delta_P = 42.1$ ppm (Figure S2e in the Supporting Information), similar to that observed with the in situ system. No new species were generated during the heating period, and the final RT $^{31}P\{^1H\}$ NMR spectrum was identical to that measured initially (Figure S2a and f in the Supporting Information). When this $^{31}P\{^1H\}$ NMR spectra measured at RT is compared with that of **11** and the initial mixture of **12**, **13** and **14**, it appears that complexes **11**–**14** constitute the major species in the mixture (Figure S3 in the Supporting Information).

At lower temperatures, the fluxionality of these complexes could be slowed down to attain more defined resonances. In the measured $^{31}P\{^1H\}$ NMR spectra, the major species were identified as **11** (doublet at $\delta_P = 40.3$ ppm and triplet at $\delta_P = 46.8$ ppm, Figure 6b–e, thick arrow). In addition, a weak singlet at $\delta_P = 38.5$ ppm could be assigned to **12** (Figure 6b–e, dot in cicle), whereas a triplet at $\delta_P = 41.1$ ppm coupled to a doublet at $\delta_P = 50.0$ ppm ($^2J_{PP} = 42.6$ Hz; Figure 6d and e, thin arrow) could be assigned tentatively to complex **13**. No hydride resonances were detected in the ^1H NMR spectra. Although unambiguous assignments of all the observed species could not be made, it seems plausible that the mixture largely consists of the Ru^{II} triphos complexes **11**–**13** in which one or more of the coordination sites is occupied by a methanesulfonato group, coordinated in either a mono- or a bidentate fashion. The nuclearities of these complexes (i.e., monomeric vs. dimeric) strongly depend on the conditions, such as the metal precursor employed, the acid to precursor ratio and the time spent in solution.

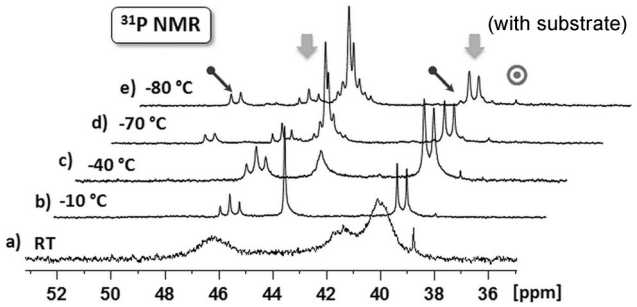

Figure 6. $^{31}P\{^1H\}$ VT-HP NMR spectra recorded for a solution of *N*-phenylacetamide (0.75 mmol), [D_8]THF (3 mL), **9** (10 mol%) and MSA (15 mol%) under H_2 (10 bar), where thick arrow, dot in circle and thin arrow indicate resonances corresponding to **11**, **12** and **13**, respectively.

The presence of MSA thus appears to be necessary for the formation of these hydride-free species containing one of more weakly coordinated methanesulfonato ligands, which presumably provide an entry into the catalytic cycle upon reaction with H_2 and substrate. Similar species are observed in the absence of substrate along with a doublet at $\delta_P = 41.9$ ppm coupled to a triplet at $\delta_P = 30.0$ ppm assigned to [Ru(CH_3SO_3-κ^1O)(CH_3SO_3-κ^2O,O′)triphos] (**14**; Figure 7d and e, star).

Given that the hydride ligand in **9** is immediately lost as H_2 in the presence of MSA, the diacetate analogue, [Ru(OAc-κ^1O)(OAc-κ^2O,O′)(triphos)] (**15**), was investigated as a completely hydride free precatalyst. The solution behav-

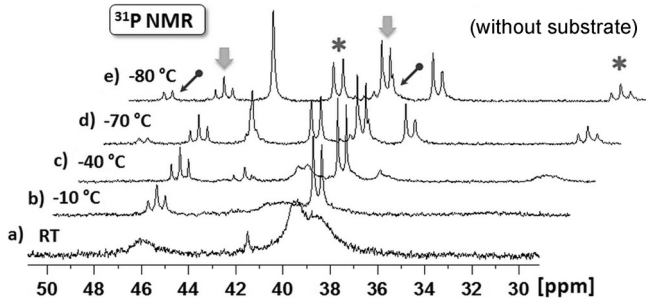

Figure 7. $^{31}P\{^{1}H\}$ VT-HP NMR spectra recorded for a solution of **9** and MSA (1.5 equiv) in $[D_8]$THF under a H_2 pressure of 10 bar, where thick arrow, thin arrow and star indicate resonances corresponding to **11**, **13** and **14**, respectively.

iour of **15** in the presence of 1 or 2 equiv of MSA is analogous to that of **9**, giving **11** or a mixture of **12**–**14**, respectively. Most significantly, the catalytic reactivity pattern of **15** is in line with that observed for **9** and the in situ system, reducing the secondary *N*-phenylacetamide preferentially over its tertiary congener (Table 5). The catalytic performance

Table 5. Amide hydrogenations with [Ru(OAc-κ^1O)(OAc-κ^2O,O′)-(triphos)] (**15**) as precatalyst.[a]

Entry	Substrate	MSA [mol%]	P_{H_2} [bar][b]	t [h]	Conv. [%]	Sel. [%]
1	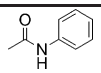	1.5	15	16	100	79
2		1.5	15	16	31	57

[a] Conditions: substrate (5 mmol), **15** (1 mol%), THF (10 mL) at 210 °C in a Hastelloy™ autoclave (250 mL). [b] At RT.

for the formation of **3** of **9** (conv. 100%, sel. 78%) and **15** (conv. 100%, sel. 79%) are identical, but deviate slightly from that of the original $[Ru(acac)_3]$/triphos system under the standard conditions (1.5 equiv MSA, conv. 100%, sel. 92%).

Given the strong influence of the MSA/Ru ratio on the activity of the in situ system, the catalytic performance of **15** was assessed over a range of MSA concentrations using *N*-phenylacetamide as the model substrate (Figure 8). It is noteworthy that even in the absence of added MSA, **15** gives 68% selectivity to the desired *N*-ethylaniline (**6**, R = Me; Figure 8). The optimum performance is obtained at a slightly lower MSA concentration (1 mol%) when compared with the 1.5 mol% required by the $[Ru(acac)_3]$/triphos system, giving full conversion with 86% selectivity towards the secondary amine. These results compare well with the original $[Ru(acac)_3]$/triphos system under the same pressure and heating conditions (conv. 100%, sel. 86%). Almost identical effects of the acid additive were observed when the isolated complex **11** was used as the catalyst precursor. Without added MSA, *N*-phenylacetamide was hydrogenated to *N*-ethylaniline, **3** (R = Me; R′ = Ph), with 93% conversion

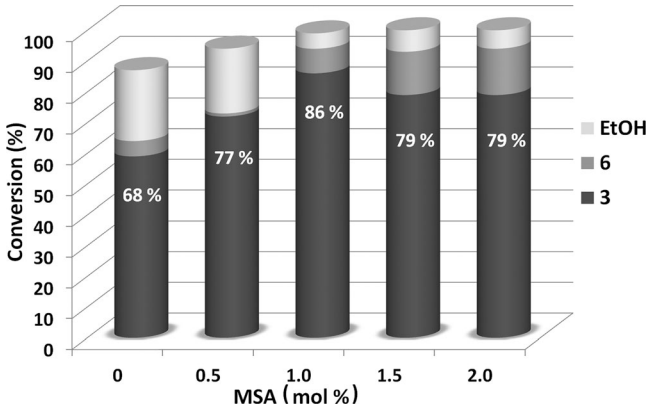

Figure 8. Effect of increasing [MSA] on the hydrogenation of *N*-phenylacetamide with [Ru(OAc-κ^1O)(OAc-κ^2O,O′)(triphos)] (**15**). Conditions: *N*-phenylacetamide (**1**, R = Me; R′ = Ph, 5 mmol), **15** (1 mol%), 210 °C, H_2 (15 bar), THF, 16 h.

and 83% selectivity after 16 h. At the shorter reaction time of 3.5 h, only 55% conversion was still obtained using **11** with no added MSA, whereas the **15**/MSA (1 equiv) system gave 96% conversion over the same period of time. These observations clearly indicate that MSA is not essential for catalysis, but plays an important role in both the formation of the active species and maintaining efficient catalytic turnover.

As mentioned previously, $[Ru(H)_2CO(triphos)]$ (**10**) was detected as one of the major species present at the end of successful catalytic hydrogenations with **9** as precatalyst (Figure 5). Using complex **10** as precatalyst, the catalytic performance in the hydrogenation of primary, secondary and tertiary amides again followed the previously observed trends (Table 6). Full conversion of the primary amide, buta-

Table 6. Amide hydrogenation with $[Ru(H)_2CO(triphos)]$ (**10**) as precatalyst.[a]

Entry	Substrate	MSA [mol%]	P_{H_2} [bar][b]	t [h]	Conv. [%]	Sel. [%]
1[c]		1.5	15	16	100	26
2		1.5	15	16	100	74
3		1.5	15	16	0	0

[a] Conditions: substrate (5 mmol), **10** (1 mol%), THF (10 mL), 210 °C in a Hastelloy™ autoclave (250 mL). [b] At RT. [c] Reaction performed in the presence of aq. NH_3 (5 mL).

namide, could be achieved with **10**, albeit the selectivity towards the primary amine, *n*-butylamine (26%) was significantly lower than with the in situ system, giving *n*-butanol, dibutylamine and tributylamine as the major side products (Table 6, entry 1). In the case of *N*-phenylacetamide, the results were comparable to those previously obtained with precatalysts **9** and **15** under the same conditions (Table 6,

entry 2). No conversion was observed with the tertiary amide, 1-methylpyrrolidin-2-one, as substrate (Table 6, entry 3).

To evaluate the stability of **10** under catalytic conditions, a solution of *N*-phenylacetamide and **10** in [D_8]THF was treated with MSA (1.5 mol%), pressurised to 10 bar with H_2 in a sapphire NMR cell and subjected to VT-HP NMR spectroscopy (Scheme 3a; Figure 9). From the initial $^{31}P\{^1H\}$ spectrum recorded at RT it is evident that, in the presence of MSA, one hydride ligand is lost immediately as hydrogen to give the methanesulfonato monohydride complex [RuH(CO)(CH_3SO_3-κ^1O)(triphos)] (**16**) as the major product, giving rise to three doublets of doublets at $\delta_P = 2.8$, 16.8 and 52.9 ppm ($^2J_{PP} = 28.6$, 18.5 and 42.1 Hz; Figure 9a).

Interestingly, a sharp singlet observed at $\delta_P = 42.9$ ppm could be assigned to the dimeric Ru(I) complex, [{Ru(μ-H)(triphos)}$_2$] (**18**), containing two bridging hydride ligands and a formal Ru–Ru bond. Serendipitously, this complex was obtained earlier as the major side-product during the preparation of **10** and fully characterised. The structure could be confirmed by X-ray diffraction and its formation also occurs in other hydrogenation reactions using the Ru/triphos system.[11] In addition to **18**, minor amounts of **12** and **13** were also observed at $\delta_P = 42.2$ ppm (bs).

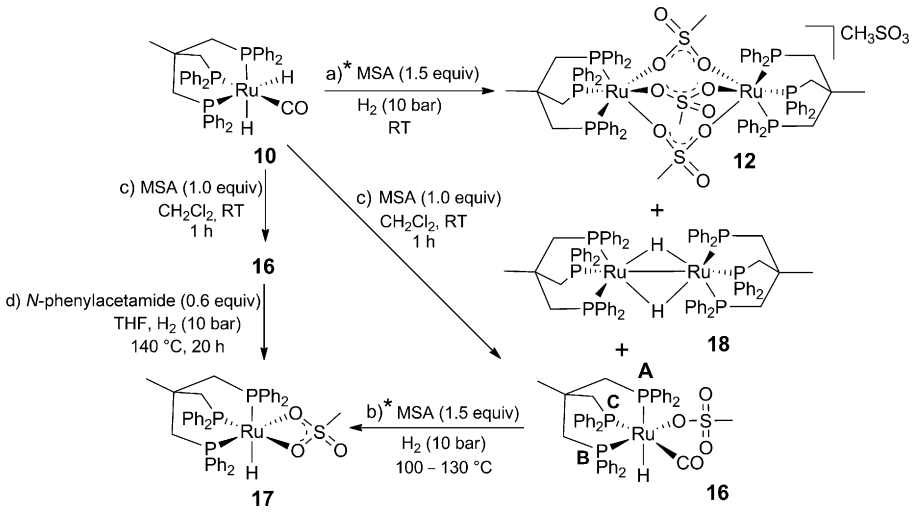

Scheme 3. Products observed during reactions of **10** with MSA; *: observed in situ during VT-HP NMR studies.

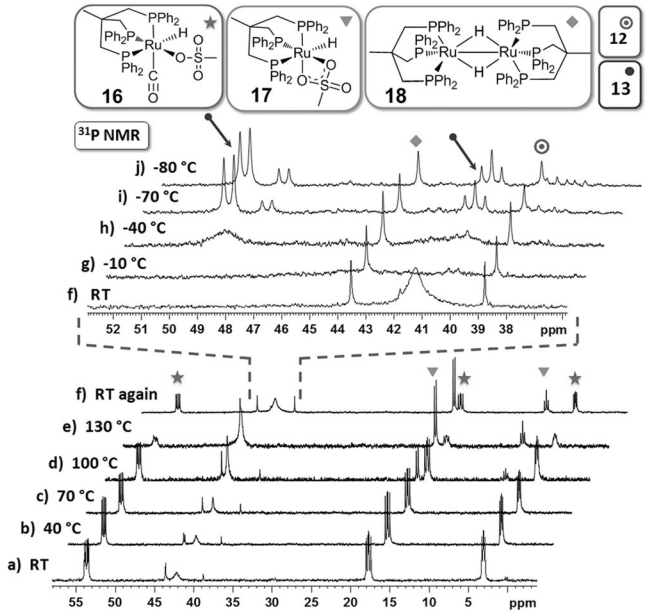

Figure 9. $^{31}P\{^1H\}$ NMR spectra recorded during a VT HP NMR study on the in solution behaviour of **10**. Conditions: *N*-phenylacetamide (0.75 mmol), [D_8]THF (3 mL), **10** (10 mol%), MSA (15 mol%) and H_2 (10 bar).

At higher temperatures (≥ 100°C), **16** was gradually converted to the bidentate methanesulfonato complex [RuH(CH_3SO_3-κ^2O,O′)(triphos)] (**17**) with loss of CO. The latter gives rise to a triplet and a doublet at $\delta_P = 6.7$ and 18.5 ppm ($^2J_{PP} = 28.1$ Hz), respectively, in the ^{31}P NMR spectrum (Figure 9d–f). Also, in the ^1H NMR spectrum a doublet of triplets at $\delta_H = -6.71$ ppm ($^2J_{HP}^{trans} = 64.6$ Hz, $^2J_{HP}^{cis} = 15.5$ Hz) could be assigned to the hydride ligand. Complex **16** could also be prepared and characterised independently by treating a solution of **10** in dichloromethane with 1 equiv of MSA at RT (Scheme 3c). Similarly, complex **17** (~20%) could be generated by heating isolated **16** and *N*-phenylacetamide (0.6 equiv) in THF at 150°C under an atmosphere of H_2 (10 bar) for 20 h (Scheme 3d).

As mentioned before, the VT-HP NMR experiments were performed at significantly lower temperatures than the standard catalytic conditions (130 vs. 210°C) owing to instrumental limitations. It is noteworthy that some minor conversion (~2.5%) was still achieved during VT-HP NMR experiments with **10**. It is thus plausible that one of the detected hydride complexes represents the most direct entry into the catalytic cycle.

Interestingly, the optimal MSA concentration (0.5 mol%, Figure 10) for reactions with **10** was found to be significantly lower than what was required for successful *N*-phenylacetamide hydrogenation with either [Ru(acac)$_3$]/triphos (1.5 mol%, Figure 1) or precatalyst **15** (1.0 mol%, Figure 8). Moreover, $^{31}P\{^1H\}$ NMR spectra of the product mixture at the end of catalytic reactions with **10** at MSA concentrations of up to 1 mol% still display the presence of significant amounts of **10**. In addition to **10**, the earlier observed Ru(I) dimer **18** is also present with the relative ratio of **18** to **10** increasing with increases in the MSA concentration until finally only **18** is observed at MSA concentrations above

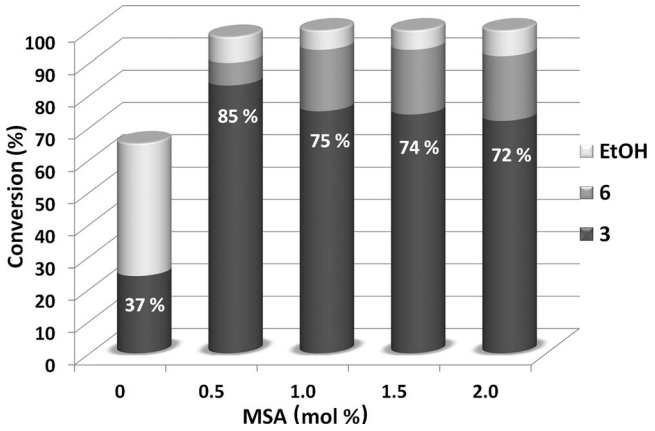

Figure 10. Effect of increasing [MSA] on the products of hydrogenation of *N*-phenylacetamide with $[Ru(H)_2CO(triphos)]$ (**10**) as precatalyst. *N*-Phenylacetamide (**1**, R = Me; R′ = Ph, 5 mmol), **10** (1 mol%), MSA (0–2.0 mol%), 210 °C, H_2 (15 bar), THF (10 mL), 16 h.

1 mol%. Catalytic hydrogenations with isolated **18** as precatalyst and 1 mol% MSA per Ru gave no reaction, suggesting that the formation of **18**, which cannot be reactivated, most likely defines a major deactivation pathway.

Mechanistic proposal: We can now tentatively identify all the species observed with the in situ catalyst after heating the $[Ru(acac)_3]$/triphos system with MSA in THF under hydrogen (Figure 3). From low temperature $^{31}P\{^1H\}$ NMR spectra, it is evident that the mixture largely consists of complex **14** (Figure 3c, star). Furthermore, the Ru^{II}–triphos complexes containing the MSA anion **12** (dot in circle) and **13** (thin arrow) are observed at −80 °C. The only hydride species in solution **18** (diamond) is present in trace amounts. Since control experiments have shown **18** to be catalytically inactive, only complexes **12–14** may be regarded as possible catalytically important species in this mixture. These complexes can be regarded as various isomeric forms of the species $[Ru(CH_3SO_3)_2(triphos)]$, which are in a dynamic concentration and temperature dependent equilibrium.

Consistent with all experimental results so far, a reasonable scenario involves this "pool" **12–14** as the direct precursor to the active species, reacting with H_2 and the substrate to enter the catalytic cycle. The cationic monohydride complexes **16** and **17** provide plausible candidates for this entry point based on the experimental results obtained since they are formed when $[Ru(H)_2CO(triphos)]$ (**10**) is treated with MSA. Compound **10** is also observed in some post-catalytic solutions when using the catalyst formed in situ from $[Ru(acac)_3]$, triphos and MSA. However, the direct activation of dihydrogen molecules at the highly Lewis acidic Ru^{II} centres in **12–14** appears equally possible and a final conclusion cannot be drawn as yet.

In both cases, the acidic additive MSA appears to have a dual role: 1) it provides a weakly coordinating counterion that allows sufficient stabilisation of the Ru^{II}–triphos fragment without blocking the generation of the active species; 2) it provides a balanced pK_a in the reaction medium to control the necessary H-transfer and hydrolytic steps within the complex reaction sequence. The resulting subtle interplay of acid and metal catalyst explains the significant variation of the optimum MSA/precursor ratio with the various precatalysts.

Conclusion

A new catalytic system has been developed for the homogeneous hydrogenation of amides to the corresponding amines. It can be conveniently generated in situ from $[Ru(acac)_3]$ and the triphos ligand together with catalytic quantities of MSA. Hydrogen pressures as low as 10 bar can be employed at temperatures around 200–210 °C. The system works very well for *N*-aromatic secondary amides, such as *N*-phenylacetamide. It also provides access to primary amines from amides, such as butanamide, and allows reduction of certain tertiary amides. In particular, it allows for the first-time hydrogenation of aromatic amides to amines without any competing arene hydrogenation or C–N bond cleavage.

A detailed high pressure NMR study of the organometallic species present in the reaction solutions arising from the in situ catalyst, as well as from isolated Ru^{II} complexes of the triphos ligand, revealed the presence of a range of complexes containing coordinated monodentate or chelating $[CH_3SO_3]^-$. Several of these species could be isolated and structurally characterised by single crystal X-ray diffraction. None of these complexes contain hydrides, and the main component in solution is proposed to be $[Ru(CH_3SO_3\text{-}\kappa^1O)(CH_3SO_3\text{-}\kappa^2O,O')(triphos)]$, which is in equilibrium with its dimeric analogue, $[Ru_2(\mu\text{-}CH_3SO_3)_3(triphos)][CH_3SO_3]$. These species are active in their own right even in the absence of added MSA. The only Ru hydride species that are seen in post-catalytic reaction solutions are the dihydrido Ru^{II} complex $[Ru(H)_2CO(triphos)]$ and the Ru(I) dimer, $[Ru(\mu\text{-}H)(triphos)]_2$. The Ru(I) dimer is not itself catalytically active and may thus represent an important deactivation pathway for the catalyst.

The obtained data are consistent with the assumption that the equilibrium mixture of the various MSA complexes act as a pool or reservoir for the $[(triphos)Ru]^{2+}$ fragment as the entry point into the actual cycle upon reaction with H_2 and substrate. Formation of hydride complexes or direct heterolytic cleavage of the H_2 molecule remains equally plausible at this stage. The function of the acidic additive, MSA, in these reactions is not only to generate the active catalytic species, but also to control the protonation–deprotonation sequences required for efficient catalytic turnover. Although the exact nature of the individual intermediates in the catalytic cycle remains, as yet, elusive, these data provide important guidelines for rational further development of the catalytic system. Therefore, the Ru/triphos system provides a promising approach towards efficient catalytic reduction of amides with molecular hydrogen, and can thus have a major

impact on sustainable production of amines from amides in the pharmaceutical industry.

Experimental Section

General materials and methods: All reactions were carried out under an inert atmosphere of N_2 (N_2, passed through a column of Cr(II) adsorbed on silica) unless otherwise stated, using standard Schlenk and vacuum-line techniques or in a glovebox when necessary. [Ru(acac)$_3$], triphos, methanesulfonic acid, diphenylamine, acetyl chloride and aniline were purchased from Aldrich and used as received. *N*-Phenylacetamide, benzanilide, benzoyl chloride, *p*-anisoyl chloride and *N*-(*p*-tolylacetamide) were purchased from Acros organics; *p*-toluoyl chloride, benzylamine, *N*-methylbenzamide, *N*,*N*-dimethylbenzamide, *N*-methyl-*N*-phenylbenzamide, 1-methylpyrrolidin-2-one, 1-phenylpyrrolidin-2-one were from Alfa Aesar and butanamide from Fluka. Aqueous ammonia (35%) and tetrahydrofuran were purchased from Fisher Scientific; *N*-(4-methoxyphenyl)acetamide and *N*,*N*-diphenylacetamide were purchased from TCI Europe. *N*-(4-Fluorophenyl)acetamide was purchased from Apollo Scientific. Amide substrates not listed here were prepared using standard literature procedures; more details can be found in the Supporting Information. Gases were supplied by BOC.

[$Ru_2(\mu$-Cl)$_3$(triphos)$_2$]Cl,[12] [Ru(H)(BH$_4$)(triphos)],[13] [Ru(H)$_2$CO(triphos)],[9g] [Ru(H)(OAc-κ^2O,O′)(PPh$_3$)$_3$],[14] [Ru(H)(OAc-κ^2O,O′)(triphos)][15] were prepared using standard literature procedures. All amide substrates were purified by recrystallisation (typically from toluene) prior to use. Toluene and tetrahydrofuran were dried using a Braun solvent purification system and used without any further degassing steps.

NMR spectra were recorded on a Bruker Avance 300 FT or Bruker Avance II 400 MHz spectrometer (^{1}H NMR at 300/400 MHz and ^{13}C{^{1}H} NMR at 75/100 MHz) with chemical shifts reported relative to tetramethylsilane (TMS). ^{1}H and ^{13}C{^{1}H} NMR spectra were referenced internally to deuterated solvent resonances, which were referenced relative to TMS. In situ VT-HP NMR studies were performed using a sapphire NMR cell purchased from Hydraulik und Industrie-Technik GmbH.

Solid state IR spectra were recorded using pressed KBr pellets on a Perkin–Elmer Spectrum GX IR spectrometer. Elemental analysis was performed by London Metropolitan University. Melting points were determined on a Gallenkamp apparatus and are uncorrected. GC-MS chromatograms were recorded on a Hewlett–Packard 6890 series GC system equipped with an Agilent J&W HP-1 general purpose column (fused silica capillary) and an HP 5973 Mass selective detector for both qualitative (MS) and quantitative (FID) analysis. A Hewlett–Packard Chemstation allowed for the computerised integration of peak areas. Method: flow rate 1 mL min^{-1} (He carrier gas), split ratio 100:1, starting temperature 50 °C (4 min) ramp rate 20 °C min^{-1} to 130 °C (2 min), ramp rate 20 °C min^{-1} to 220 °C (15.5 min).

Catalysis, synthesis and VT-HP NMR spectroscopy

General procedure for catalytic batch reactions with [Ru(acac)$_3$]/triphos or precatalysts 9–15: [Ru(acac)$_3$] (0.02 g, 0.05 mmol, 1 mol%) and triphos (0.062 g, 0.10 mmol, 2 mol%) or one of the precatalysts **9–15** (0.05 mmol, 1 mol%) were added to a Hastelloy™ autoclave fitted with a stirrer bar, in air. An amide substrate (5 mmol) was added and the autoclave was subsequently sealed and purged by three vacuum/N_2 cycles using a Schlenk line. A septum was fitted and dry, degassed THF (10 mL) was introduced by using a syringe. In the case of addition of acid, a solution of methanesulfonic acid (3–4.87 μL, 0.05–0.075 mmol, 1–1.5 mol%) in THF (10 mL) was added to the autoclave instead. For primary amides aqueous ammonia (5 mL) was also added to the autoclave. The autoclave was sealed again, purged (~10 bar H_2, six times), pressure tested (40–50 bar of H_2) and then pressurised with H_2 (10–40 bar). The autoclave was then heated with stirring to an internal temperature of 200–220 °C using an external heating jacket for 4–16 h. At the end of the reaction, the autoclave was cooled rapidly by immersing it in cold water. After venting the autoclave to the atmosphere in a well-ventilated fume-hood, the content was sampled under an inert atmosphere prior to transferral of the remaining content to a sample vial, in air. The crude mixtures were analysed using GC-MS, GC-FID and NMR spectroscopy. Quantitative calculations were based on recorded ^{1}H NMR spectra unless otherwise stated.

[Ru(CH$_3$SO$_3$-κ^1O)(OAc-κ^2O,O′)(triphos)] (11): Methanesulfonic acid (5.5 mg, 0.06 mmol, 3.7 μL) was added with a microsyringe to a suspension of [RuH(OAc-κ^2O,O′)(triphos)] (0.05 g, 0.06 mmol) or [Ru(OAc-κ^1O)(OAc-κ^2O,O′)(triphos)] (0.05 g, 0.06 mmol) in THF (1.5 mL). The resulting mixture was then allowed to stir at RT for 1 h. All volatiles were subsequently removed under reduced pressure. The crude yellow residue was washed with hexane (6 mL) and dried in vacuo to give the pure product as a yellow solid (49.0 mg, 98%). Single crystals of **11** suitable for analysis by X-ray diffraction could be obtained by slow diffusion of hexane into a solution of **11** in dichloromethane at RT. M.p. 260–265 °C (decompose). ^{1}H NMR (400 MHz, CD_2Cl_2, 25 °C): δ_H = 1.57 (q, 3H, $^4J_{HP}$ = 2.7 Hz; −CH_3), 1.98 (s, 3H, −C(O)CH_3), 2.27 (bs, 6H, −CH_2−), 2.46 (bs, 3H, −SCH_3), 6.88–7.79 ppm (m, 30H, Ph); ^{13}C{^{1}H} NMR (100 MHz, CD_2Cl_2, 25 °C): δ_C = 26.1 (s, −C(O)CH_3), 32.6 (m, −CH_2−), 37.8 (q, $^3J_{CP}$ = 11.1 Hz, −CH_3), 38.4 (q, $^2J_{CP}$ = 2.8 Hz, −C(CH$_2$PPh$_2$)$_3$), 41.3 (s, −SO$_3$CH_3), 128.1 (m, Ph^{meta}), 129.5 (s, Ph^{para}), 132.5 (m, Ph^{ortho}), signal too weak (Ph^{ipso}), 190.3 ppm (s, −C(O)CH$_3$); ^{31}P{^{1}H} NMR (161 MHz, CD_2Cl_2, 25 °C): δ_P = 39.4 (bd, 2P, J_{PP} = 43.2 Hz, −*P*Ph), 45.3 ppm (bt, 1P, J_{PP} = 43.2 Hz, −*P*Ph); ^{31}P{^{1}H} NMR (121 MHz, [D$_8$]THF, −40 °C): δ_P = 40.3 (d, 2P, J_{PP} = 43.2 Hz, −*P*Ph), 46.8 ppm (t, 1P, J_{PP} = 43.2 Hz, −*P*Ph); IR (KBr): $\tilde{\nu}$ = 3054 [w, sp^2 ν(C−H)], 2921–2850 [w, sp^3 ν(C−H)], 1461 [st, ν(κ^2-OCO$_{sym}$)], 1434 [st, ν(P−Ph)], 1247–1156 cm^{-1} [st, ν(SO)]; elemental analysis (%): found: C 57.98, H 5.15; $C_{44}H_{45}O_5P_3RuS$ requires: C 60.06, H 5.15; for $C_{44}H_{45}O_5P_3RuS{\cdot}H_2O$: C 58.86, H 5.28.

Mixture of [Ru$_2$(μ-CH$_3$SO$_3$)$_3$(triphos)$_2$]CH$_3$SO$_3$ (12), H[Ru(CH$_3$SO$_3$-κ^1O)$_3$(triphos)] (13) and [Ru(CH$_3$SO$_3$-κ^1O)(CH$_3$SO$_3$-κ^2O,O′)(triphos)] (14): Methanesulfonic acid (9.5 mg, 0.10 mmol, 6.4 μL) was added with a microsyringe to a suspension of [RuH(OAc-κ^2O,O′)(triphos)] (0.04 g, 0.05 mmol) or [Ru(OAc-κ^1O)(OAc-κ^2O,O′)(triphos)] (0.04 g, 0.05 mmol) in THF (1.5 mL). The resulting mixture was then allowed to stir at RT for 1 h. All volatiles were subsequently removed under reduced pressure. The crude yellow residue was washed with hexane (6 mL) and dried in vacuo to give a mixture initially (0.50 g) of **13**+**14** (57%) and **12** (43%) as a bright yellow solid. This mixture, if left standing in solution, equilibrates over a time to give largely **14** after a period of 5–6 days. Single crystals of **12** suitable for analysis by X-ray diffraction could be obtained by slow diffusion of hexane into a solution of the mixture in dichloromethane at RT. IR (KBr) for the mixture: $\tilde{\nu}$ = 3049 [m, sp^2 ν(C−H)], 2955–2871 [m, sp^3 ν(C−H)], 1434 [st, ν(P−Ph)], 1235–1051 cm^{-1} [st, ν(−SO$_3$)].

For [Ru$_2$(μ-CH$_3$SO$_3$)$_3$(triphos)$_2$][CH$_3$SO$_3$] (12):[16] ^{1}H NMR (400 MHz, CD_2Cl_2, 25 °C): δ_H = 1.55 (m, 6H, −CH_3), 1.99 (s, 3H, −SCH_3), 2.17 (s, 9H, −SCH_3), 2.22 (m, 6H, −CH_2−), 2.43 (m, 6H, −CH_2−), 6.97–7.64 ppm (m, 60H, Ph); ^{31}P{^{1}H} NMR (161 MHz, CD_2Cl_2, 25 °C): δ_P = 38.5 ppm (bs, 6P, −*P*Ph); elemental analysis (%): found: C 56.20, H 5.08; $C_{86}H_{90}O_{12}P_6Ru_2S_4$ requires: C 56.39, H 4.95.

For H[Ru(CH$_3$SO$_3$-κ^1O)$_3$(triphos)] (13): This complex could also be prepared independently by the addition of methanesulfonic acid (79.0 mg, 0.82 mmol, 0.05 mL) with a microsyringe to a solution of [Ru(OAc-κ^1O)(OAc-κ^2O,O′)(triphos)] (0.14 g, 0.16 mmol) in dichloromethane (2.0 mL) at RT. The resulting orange mixture was then allowed to stir at RT for 1 h after which the crude mixture was analysed by NMR spectroscopy. This complex appears only to exist in the presence of an excess of MSA as all attempts to isolate this complex resulted in the isolation of a mixture of **12** and **14** instead. ^{1}H NMR (300 MHz, CD_2Cl_2, 25 °C): δ_H = 1.80 (bs, 3H, −CH_3), 2.50 (s, 6H, −CH_2−), 3.10 (bs, 9H, −SCH_3), 7.12 (t, 12H, $^3J_{HP}$ = 7.9 Hz, Ph), 7.30 ppm (t, 18H, $^3J_{HP}$ = 7.9 Hz, Ph); ^{13}C{^{1}H} NMR (75 MHz, CD_2Cl_2, 25 °C): δ_C = 22.7 (s, −C(CH$_2$PPh$_2$)$_3$), 32.1 (m, −CH_2−), 36.1 (q, $^3J_{CP}$ = 11.6 Hz, −CH_3), 39.3 (s, −SO$_3$CH_3), 128.8 (m, Ph^{meta}), 130.9 (s, Ph^{para}), 131.8 (m, Ph^{ortho}), 132.4 ppm (m, Ph^{ipso}); ^{31}P{^{1}H} NMR (121 MHz, CD_2Cl_2, 25 °C): δ_P = 48.5 ppm (bs, 3P, −*P*Ph); ^{31}P{^{1}H} NMR (121 MHz, [D$_8$]THF, −80 °C): δ_P = 41.1 (t, 1P, $^2J_{PP}$ = 42.6 Hz, −*P*Ph), 50.0 ppm (d, 2P, $^2J_{PP}$ = 42.6 Hz, −*P*Ph).

For [Ru(CH_3SO_3-κ^{1}O)(CH_3SO_3-κ^{2}O,O′)(triphos)] (14):[16] ^{1}H NMR (300 MHz, CD_2Cl_2, 25 °C): δ_H = 1.55 (m, 3H, −CH_3), 2.34 (m, 6H, −CH_2−), 2.68 (s, 6H, −SCH_3), 7.06–7.64 ppm (m, 30H, Ph); ^{13}C{^{1}H} NMR (100 MHz, CD_2Cl_2, 25 °C): δ_C = 33.0 (m, −CH_2−), 37.7 (m, −CH_3), 38.0 (s, −C(CH_2PPh_2)$_3$), 40.5 (s, −SO_3CH_3), 128.6 (m, Ph^{meta}), 130.1 (s, Ph^{para}), 132.9 (m, Ph^{ortho}), 135.2 ppm (d, $^1J_{CP}$ = 45.4 Hz, Ph^{ipso}); ^{31}P{^{1}H} NMR (121 MHz, CD_2Cl_2, 25 °C): δ_P = 38.7 ppm (bs, 3P, −PPh); ^{31}P{^{1}H} NMR (121 MHz, CD_2Cl_2, −80 °C): δ_P = 29.1 (t, 1P, $^2J_{PP}$ = 48.8 Hz, −PPh), 42.9 ppm (d, 2P, $^2J_{PP}$ = 48.8 Hz, −PPh); ^{31}P{^{1}H} NMR (121 MHz, [D_8]THF, −80 °C): δ_P = 30.0 (t, 1P, $^2J_{PP}$ = 48.8 Hz, −PPh), 41.9 ppm (d, 2P, $^2J_{PP}$ = 48.8 Hz, −PPh). During an attempt to isolate **14** by crystallisation, crystals of the water coordinated analogue [Ru(CH_3SO_3)$_2$(H_2O)(triphos)] (**19**) were isolated instead.

For [Ru(CH_3SO_3-κ^{1}O)$_2$(H_2O)(triphos)] (19): ^{1}H NMR (300 MHz, [D_8]THF, 25 °C): δ_H = 1.54 (m, 3H, −CH_3), 2.39 (m, 6H, −CH_2−), 2.57 (s, 6H, −SCH_3), 7.05–7.58 ppm (m, 30H, Ph); ^{31}P{^{1}H} NMR (121 MHz, [D_8]THF, 25 °C): δ_P = 38.4 ppm (bs, 3P, −PPh); ^{31}P{^{1}H} NMR (121 MHz, [D_8]THF, −80 °C): δ_P = 37.3 (d, 2P, J_{PP} = 47.0 Hz, −PPh), 40.2 ppm (t, 1P, J_{PP} = 47.0 Hz, −PPh).

[Ru(OAc-κ^{1}O)(OAc-κ^{2}O,O′)(PPh_3)$_3$]: A suspension of [$RuCl_2$(PPh_3)$_3$] (7.2 g, 7.5 mmol) in methanol (250 mL) was treated with a solution of NaOAc·3H_2O (10.6 g, 106.3 mmol) in methanol (5 mL). The resulting mixture was then refluxed at 75 °C for 75 min with stirring. The mixture was subsequently slowly cooled to 0 °C and the orange solid, which precipitated from solution, was collected in air, washed with ethanol (2× 25 mL) and dried, overnight, in vacuo to obtain the pure product as an orange microcrystalline solid (5.8 g, 78 %). ^{1}H NMR (300 MHz, CD_2Cl_2, 25 °C): δ_H = 1.48 (s, 6H, −C(O)CH_3), 6.90–7.32 ppm (m, 45H, Ph); ^{31}P{^{1}H} NMR (121 MHz, CD_2Cl_2, 25 °C): δ_P = 63.8 ppm (s). These data are consistent with those from the literature.[17]

[Ru(OAc-κ^{1}O)(OAc-κ^{2}O,O′)(triphos)] (15): A suspension of [Ru(OAc-κ^{1}O)(OAc-κ^{2}O,O′)(PPh_3)$_3$] (5.8 g, 5.8 mmol) in toluene (35 mL) was treated with triphos (3.9 g, 6.2 mmol). The resulting mixture was then refluxed at 113 °C for 3 h with stirring. The mixture was subsequently slowly cooled to 0 °C and the orange solid, which precipitated from solution, was collected under an inert atmosphere of N_2, washed with toluene (2× 10 mL), diethyl ether (2× 10 mL) and dried in vacuo to obtain the pure product as an orange microcrystalline solid (3.6 g, 70 %). Single crystals of the analogous complex [Ru(OAc-κ^{1}O)$_2$(H_2O)(triphos)] (**20**) suitable for analysis by X-ray diffraction could be obtained by slow diffusion of hexane into a solution of **15** in dichloromethane at RT. For compound **15**: M.p. 249–252 °C (decomp); ^{1}H NMR (400 MHz, CD_2Cl_2, 25 °C): δ_H = 1.57 (q, 3H, $^4J_{HP}$ = 2.7 Hz, −CH_3), 1.89 (s, 6H, −C(O)CH_3), 2.20 (m, 6H, −CH_2−), 6.99 (t, 12H, $^3J_{HH}$ = 7.5 Hz, Ph^{meta}), 7.14 (t, 6H, $^3J_{HH}$ = 7.5 Hz, Ph^{para}), 7.40 ppm (m, 12H, Ph^{ortho}); ^{13}C{^{1}H} NMR (100 MHz, CD_2Cl_2, 25 °C): δ_C = 25.5 (s, −C(O)CH_3), 34.3 (m, −CH_2−), 37.8 (q, $^3J_{CP}$ = 10.6 Hz, −CH_3), 38.6 (t, $^2J_{CP}$ = 3.4 Hz, −C(CH_2PPh_2)$_3$), 127.9 (m, Ph^{meta}), 129.2 (bs, Ph^{para}), 132.7 (m, Ph^{ortho}), 137.2 (m, Ph^{ipso}), 181.6 ppm (s, −C(O)−); ^{31}P{^{1}H} NMR (161 MHz, CD_2Cl_2, 25 °C): δ_P = 40.3 (s); IR (KBr): $\tilde{\nu}$ = 3049 [m, sp^2 ν(C−H)], 2921–2857 [m, sp^3 ν(C−H)], 1609 [st, ν(κ^1-OCO_{assym})], 1456 [st, ν(κ^2-OCO_{sym})], 1370 cm^{-1} [m, ν(κ^1-OCO_{sym})]; elemental analysis (%): found C 64.10, H 5.47; $C_{45}H_{45}O_4P_3Ru$ requires: C 64.05, H 5.38.

[RuH(CO)(CH_3SO_3-κ^{1}O)(triphos)] (16): Methanesulfonic acid (12.0 mg, 0.13 mmol, 8.1 μL) was added with a microsyringe to a solution of [Ru(H_2)CO(triphos)] (0.10 g, 0.13 mmol) in dichloromethane (1.5 mL). The resulting mixture was then allowed to stir at RT for 1 h. All volatiles were subsequently removed under reduced pressure and the product was dried in vacuo to give **16** as a yellow solid (0.09 mg, 81 %). M.p. 185–188 °C (decomp); ^{1}H NMR (300 MHz, CD_2Cl_2, 25 °C): δ_H = −5.56 (ddd, 1H, $^2J_{HP}^{trans}$ = 95.5 Hz, $^2J_{HP}^{cis}$ = 19.8 Hz, $^2J_{HP}^{cis}$ = 14.3 Hz, Ru-H), 1.60 (bs, 3H, −CH_3), 2.18 (m, 2H, −CH_2−), 2.31 (m, 2H, −CH_2−), 2.53 (m, 2H, −CH_2−), 2.55 (m, 3H, −SCH_3), 6.62–7.90 ppm (m, 30H, Ph); ^{13}C{^{1}H} NMR (75 MHz, CD_2Cl_2, 25 °C): δ_C = 33.0 (dt, $^1J_{CP}$ = 23.4 Hz, $^3J_{CP}$ = 5.8 Hz, −CH_2−), 33.9 (dt, $^1J_{CP}$ = 20.2 Hz, $^3J_{CP}$ = 3.6 Hz, −CH_2−), 35.7 (dt, $^1J_{CP}$ = 28.3 Hz, $^3J_{CP}$ = 5.4 Hz, −CH_2−), 38.3 (s, −C(CH_2PPh_2)$_3$), 38.6 (t, $^3J_{CP}$ = 9.4 Hz, −CH_3), 38.8 (s, −SO_3CH_3), 128.3 (m, Ph^{meta}), 129.5 (m, Ph^{para}), 131.5 (m, Ph^{ortho}), 132.8 (m, Ph^{ortho}), 133.9–139.8 (m, Ph^{ipso}), 203.3 ppm (s, CO); ^{31}P{^{1}H} NMR (121 MHz, CD_2Cl_2, 25 °C); see Scheme 3 for P atom labels: δ_P = 2.8 (dd, 1P, $^2J_{PAPB}$ = 28.6 Hz, $^2J_{PAPC}$ = 18.5 Hz, P_A), 16.8 (dd, 1P, $^2J_{PBPA}$ = 28.6 Hz, $^2J_{PBPC}$ = 42.1 Hz; P_B), 52.9 ppm (dd, 1P, $^2J_{PCPA}$ = 18.5 Hz, $^2J_{PCPB}$ = 42.1 Hz; P_C); ATR-IR: $\tilde{\nu}$ = 3053 [w, sp^2 ν(C−H)], 2945–2914 [w, sp^3 ν(C−H)], 1979 [st, ν(CO)], 1904 [w, ν(Ru−H)], 1435 [m, ν(P−Ph)], 1246, 1151, 1030 cm^{-1} [st, ν(κ^1-SO_3CH_3)]; elemental analysis (%): found: C 60.88, H 5.17; $C_{43}H_{43}O_4P_3RuS$ requires: C 60.77, H 5.10.

[Ru_2(μ-H)$_2$(triphos)$_2$] (18): Following a published procedure for the synthesis of [RuH_2(CO)(triphos)],[9g] [Ru(acac)$_3$] (0.40 g, 1.0 mmol) and triphos (0.69 g, 1.1 mmol) was added to a high pressure Hastelloy™ autoclave equipped with a magnetic stirrer bar. The autoclave was sealed and purged by three vacuum/N_2 cycles. Degassed propanal (10 mL) was added to the autoclave under a flow of nitrogen. The autoclave was then sealed, purged with H_2 (3× 20 bar) and finally pressurised with H_2 to 90 bar. After stirring at 150 °C for 20 h, the autoclave was cooled to 0 °C, and vented to the atmosphere in a well-ventilated fume-hood. The orange product mixture was transferred to a Schlenk flask and ethanol (20 mL) added to the mixture to precipitate the formed by-product [Ru(H)$_2$CO(triphos)] as a white solid. Removal of the [Ru(H)$_2$CO-(triphos)] by filtration gave a bright orange filtrate from which the title product could be precipitated by addition of hexane (70 mL). The orange solid was collected, washed with hexane (2× 10 mL) and recrystallised from dichloromethane layered with hexane as bright orange crystals (1.0 g, 70 %). Single crystals of **18** suitable for X-ray diffraction could be obtained as orange platelets by the same method of crystallisation. M.p. 210–215 °C (decompose); ^{1}H NMR (400 MHz, CD_2Cl_2, 25 °C): δ_H = −8.84 (vt, 2H, −RuH), 1.52 (bs, 6H, −CH_3), 2.26 ppm (bs, 12H, −CH_2−); ^{13}C{^{1}H} NMR (100 MHz, CD_2Cl_2, 25 °C): δ_C = 34.4 (m, −CH_2−), 37.4 (m, −CH_3), 37.8 (s, −C(CH_2PPh_2)$_3$), 127.6 (s, Ph^{meta}), 129.2 (s, Ph^{para}), 132.5 (s, Ph^{ortho}), 138.3 ppm (bm, Ph^{ipso}); ^{31}P{^{1}H} NMR (161 MHz, CD_2Cl_2, 25 °C): δ_P = 42.9 ppm (s, 6P, −PPh); ATR-IR: $\tilde{\nu}$ = 3053 [w, sp^2 ν(C−H)], 2916–2870 [w, sp^3 ν(C−H)], 1433 cm^{-1} [st, ν(P−Ph)]; elemental analysis (%): found C 62.23, H 5.34; $C_{82}H_{80}P_6Ru_2$ requires: C 67.76, H 5.55; for $C_{82}H_{80}P_6Ru_2$·2CH_2Cl_2 (crystallisation solvent) C 62.15, H 5.22.

VT-HP NMR experiment with [Ru(acac)$_3$]/triphos in the presence of *N*-phenylacetamide, MSA and H_2: A mixture of [Ru(acac)$_3$] (0.06 g, 0.15 mmol), triphos (0.30 g, 0.19 mmol) and *N*-phenylacetamide (0.06 g, 0.45 mmol) was dissolved in [D_8]THF (3 mL) in a 20 mL Schlenk flask under an inert atmosphere of N_2. Methanesulfonic acid (14.6 μL, 0.23 mmol) was added to the solution, with stirring. The resulting red solution was then transferred to a sapphire HP NMR cell under an inert atmosphere of H_2. The solution and HP NMR cell were purged by H_2 bubbling before being sealed and pressurised to 10 bar with H_2. The reaction mixture was then analysed by HP NMR spectroscopy at temperatures 25, 60 and 130 °C. No significant change in composition of the reaction mixture was observed.

VT-HP NMR experiment with [RuH(OAc-κ^{2}O,O′)(triphos)] (9) as pre-catalyst in the presence of *N*-phenylacetamide, MSA and H_2: [RuH(OAc-κ^{2}O,O′)(triphos)] (0.06 g, 0.08 mmol) was suspended in a solution of *N*-phenylacetamide (0.10 g, 0.75 mmol) in [D_8]THF (3 mL) in a 20 mL Schlenk flask under an inert atmosphere of N_2. Methanesulfonic acid (7.3 μL, 0.11 mmol) was added to the mixture, with stirring. The resulting orange solution was then transferred to a sapphire HP NMR cell under an inert atmosphere of H_2. The solution and HP NMR cell were purged by H_2 bubbling before being sealed and pressurised to 10 bar with H_2. The reaction mixture was then analysed by HP NMR spectroscopy—first at the higher end (25 to 130 °C) and then at the lower end of the temperature range (25 to −80 °C). Species observed included compounds **11**, **12**, **13**, **14** and **18**.

VT-HP NMR experiment with [RuH(OAc-κ^{2}O,O′)(triphos)] (9) as pre-catalyst in the presence MSA and H_2 (no substrate): [RuH(OAc-κ^{2}O,O′)-(triphos)] (0.06 g, 0.08 mmol) was suspended in [D_8]THF (3 mL) in a 20 mL Schlenk flask under an inert atmosphere of N_2. Methanesulfonic acid (7.3 μL, 0.11 mmol) was added to the mixture, with stirring. The resulting orange solution was then transferred to a sapphire HP NMR cell under an inert atmosphere of H_2. The solution and HP NMR cell were purged by H_2 bubbling before being sealed and pressurised to 10 bar with H_2. The reaction mixture was then analysed by HP NMR spectroscopy—

first at the higher end (25 to 130 °C) and then at the lower end of the temperature range (25 to −80 °C). Species observed included compounds **11**, **12**, **13**, **14** and **18**.

VT-HP NMR experiment with [Ru(H)$_2$CO(triphos)] (10) as precatalyst in the presence of *N*-phenylacetamide, MSA and H$_2$: [Ru(H)$_2$CO(triphos)] (0.06 g, 0.08 mmol) was suspended in a solution of *N*-phenylacetamide (0.10 g, 0.75 mmol) in [D$_8$]THF (3 mL) in a 20 mL Schlenk flask under an inert atmosphere of N_2. Methanesulfonic acid (7.3 μL, 0.11 mmol) was added to the mixture, with stirring. The liberation of H_2 gas was visible immediately after addition of the acid in the form of bubble formation. The resulting orange solution was transferred to a sapphire HP NMR cell under an inert atmosphere of H_2. The solution and HP NMR cell were purged by H_2 bubbling before being sealed and pressurised to 10 bar with H_2. The reaction mixture was then analysed by HP NMR spectroscopy—first at the higher end (25 to 130 °C) and then at the lower end of the temperature range (25 to −80 °C). Species observed included the described compounds **12**, **16** and **18**. In addition, the formation of [RuH(SO$_3$CH$_3$-κ^{1}O)(triphos)] (**17**) was observed at temperatures ≥100 °C.

For [RuH(SO$_3$CH$_3$-κ^{2}O,O′)(triphos)] (17): Small amounts of **17** (~20% based on ^{31}P{^{1}H} integrals) could also be generated by heating a solution of **16** (0.16 g, 0.18 mmol) and *N*-phenylacetamide (0.04 g, 0.10 mmol) in THF (10 mL) in a hastelloy autoclave under an atmosphere of H_2 (10 bar) at 150 °C for 20 h. After 20 h, the autoclave was cooled to RT, vented to the atmosphere and the orange product mixture transferred to a Schlenk flask under an atmosphere of N_2. All volatiles were removed under reduced pressure to give the crude product mixture as an orange solid. All attempts to isolate **17** from the resulting mixture were unsuccessful. ^{1}H NMR (300 MHz, CH_2Cl_2, 25 °C): $\delta_H = -6.71$ (dt, 1H, $^2J_{HP}^{trans} = 64.6$ Hz, $^2J_{HP}^{cis} = 15.5$ Hz, Ru−*H*), 1.82 (m, 3H, −C*H*$_3$), 2.55 (bs, 3H, −SO$_3$C*H*$_3$), 2.66 (m, 6H, −C*H*$_2$−), 6.60–7.66 ppm (m, 30H, Ph); ^{31}P{^{1}H} NMR (121 MHz, [D$_8$]THF, 25 °C): $\delta_P = 6.7$ (t, 1P, $^2J_{PP} = 28.1$ Hz, *P*Ph), 18.5 ppm (d, 2P, $^2J_{PP} = 28.1$ Hz, *P*Ph).

X-ray crystal structure determinations: The molecular structures and tables containing a summary of the crystal data collection and refinement parameters of compounds **11**, **12**, **19** and **20** can be found in the Supporting Information. Data sets were collected on a Rigaku Mo MM007 (dual port) high brilliance diffractometer with graphite-monochromated $Mo_{K\alpha}$ radiation ($\lambda = 0.71075$ Å). The diffractometer was fitted with Saturn 70 and Mercury CCD detectors and two XStream LT accessories. Data reduction was carried out with standard methods using Rigaku CrystalClear. All the structures were solved using direct methods and conventional difference Fourier methods. All non-hydrogen atoms were refined anisotropically by full-matrix least squares calculations on F^2 using SHELXTL or SHELX-97[18] within an X-seed[19] environment. In most cases, the hydrogen atoms were fixed in calculated positions. Figure were generated with X-seed and POV Ray for Windows, with the displacement ellipsoids at 50% probability level unless stated otherwise.

CCDC-944784, CCDC-944785, CCDC-944786, and CCDC-944787 contain the supplementary crystallographic data for this paper. These data can be obtained free of charge from The Cambridge Crystallographic Data Centre via www.ccdc.cam.ac.uk/data_request/cif.

Acknowledgements

We thank the American Chemical Society, Pharmaceutical Round Table for a Postdoctoral Fellowship (D.L.D) and other support, and the European Commission for a Fellowship to J.C. The research leading to these results has received funding from the European Community's Seventh Framework Programme (FP7/2007-2013) for SYNFLOW under grant agreement no: NMP2-LA-2010-246461. Additional support from the Cluster of Excellence EC 236 "Tailor-made Fuels from Biomass" at RWTH Aachen University is also acknowledged.[5]

[1] a) E. Balaraman, B. Gnanaprakasam, L. J. W. Shimon, D. Milstein, *J. Am. Chem. Soc.* **2010**, *132*, 16756–16758; b) J. M. John, S. H. Bergens, *Angew. Chem.* **2011**, *123*, 10561–10564; *Angew. Chem. Int. Ed.* **2011**, *50*, 10377–10380; c) T. Miura, I. E. Held, S. Oishi, M. Naruto, S. Saito, *Tetahedron Lett.* **2013**, *54*, 2674–2678.

[2] S. Takebayashi, J. M. John, S. H. Bergens, *J. Am. Chem. Soc.* **2010**, *132*, 12832–12834.

[3] a) G. Beamson, A. J. Papworth, C. Philipps, A. M. Smith, R. Whyman, *J. Catal.* **2010**, *269*, 93–102; b) G. Beamson, A. J. Papworth, C. Philipps, A. M. Smith, R. Whyman, *J. Catal.* **2011**, *278*, 228–238; c) C. Hirosawa, N. Wakasa, T. Fuchikami, *Tetahedron Lett.* **1996**, *37*, 6749–6752.

[4] R. Burch, C. Paun, X. M. Cao, P. Crawford, P. Goodrich, C. Hardacre, P. Hu, L. McLaughlin, J. Sá, J. M. Thompson, *J. Catal.* **2011**, *283*, 89–97.

[5] J. Coetzee, H. G. Manyar, C. Hardacre, D. J. Cole-Hamilton, *ChemCatChem* 2013, submitted..

[6] M. Stein, B. Breit, *Angew. Chem.* **2012**, *125*, 2287–2290; *Angew. Chem. Int. Ed.* **2013**, *52*, 2231–2234.

[7] a) S. Das, B. Join, K. Junge, M. Beller, *Chem. Commun.* **2012**, *48*, 2683–2685; b) S. Das, B. Wendt, K. Möller, K. Junge, M. Beller, *Angew. Chem.* **2012**, *124*, 1694–1698; *Angew. Chem. Int. Ed.* **2012**, *51*, 1662–1666; c) S. Das, S. Zhou, D. Addis, S. Enthaler, K. Junge, M. Beller, *Top Catal.* **2010**, *53*, 979–984.

[8] D. J. C. Constable, P. J. Dunn, J. D. Hayler, G. R. Humphrey, J. L. Leazer, Jr., R. J. Linderman, K. Lorenz, J. Manley, B. A. Pearlman, A. Wells, A. Zaks, T. Y. Zhang, *Green Chem.* **2007**, *9*, 411–420.

[9] a) H. T. Teunissen, C. J. Elsevier, *Chem. Commun.* **1997**, 667–668; b) H. T. Teunissen, C. J. Elsevier, *Chem. Commun.* **1998**, 1367–1368; c) M. Kilner, D. V. Tyers, S. P. Crabtree, M. A. Wood, *PCT Int. Appl.* **2003**, WO 2003093208; d) M. A. Wood, S. P. Crabtree, D. V. Tyers, *PCT Int. Appl.* **2005**, WO 2005051875; e) M. C. van Engelen, H. T. Teunissen, J. G. de Vries, C. J. Elsevier, *J. Mol. Catal. A* **2003**, *206*, 185–192; f) F. M. A. Geilen, B. Engendahl, A. Harwardt, W. Marquardt, J. Klankermayer, W. Leitner, *Angew. Chem.* **2010**, *122*, 5642–5646; *Angew. Chem. Int. Ed.* **2010**, *49*, 5510–5514; g) F. M. A. Geilen, B. Engendahl, M. Hölscher, J. Klankermayer, W. Leitner, *J. Am. Chem. Soc.* **2011**, *133*, 14349–14358.

[10] a) A. A. Núñez Magro, G. R. Eastham, D. J. Cole-Hamilton, Chem. Commun. **2007**, 3154–3156; b) D. L. Dodds, J. Coetzee, J. Klankermayer, S. Brosinski, W. Leitner, D. J. Cole-Hamilton, *Chem. Commun.* **2012**, *48*, 12249–12262 (published additions and corrections to Ref [10a]).

[11] T. vom Stein, J. Klankermayer, W. Leitner, private correspondence, **2012**.

[12] L. F. Rhodes, C. Sorato, L. M. Venanzi, F. Bachechi, *Inorg. Chem.* **1988**, *27*, 604–610.

[13] L. F. Rhodes, L. M. Venanzi, *Inorg. Chem.* **1987**, *26*, 2692–2695.

[14] R. W. Mitchell, A. Spencer, G. Wilkinson, *J. Chem. Soc. Dalton Trans.* **1973**, 846–854.

[15] A. B. Chaplin, P. J. Dyson, *Inorg. Chem.* **2008**, *47*, 381–390.

[16] All the complexes have second order spin systems for C_{ipso} and for PCH_2. For complexes of the form [Ru(triphos)X_3]; all the C_{ipso} or CH_2 C atoms are chemically equivalent but all are magnetically inequivalent. For [Ru(triphos)X_2Y]; C_{ipso} on P *trans* to X form an ABPP′A′B′ spin system, while those on P *trans* to Y form an AA′P spin system. There may be additional coupling between the two spin systems.

[17] E. Lindner, R. Fawzi, W. Hiller, A. Carvill, M. McCann, *Chem. Ber.* **1991**, *124*, 2691–2695.

[18] SHELXL program package (version 5.1), Bruker APX Inc., Madison, WI, USA.

[19] a) L. J. Barbour, *J. Supramol. Chem.* **2001**, *1*, 189–191; b) J. L. Atwood, L. J. Barbour, *Cryst. Growth Des.* **2003**, *3*, 3–8.

Received: November 30, 2012
Revised: May 3, 2013
Published online: ■■ ■■, 0000

